Hindawi
International Journal of Antennas and Propagation
Volume 2020, Article ID 8630978, 6 pages
https://doi.org/10.1155/2020/8630978

Research Article

On the Flux Linkage between Pancake Coils in Resonance-Type Wireless Power Transfer Systems

Mauro Parise[1], **Giulio Antonini**[2], and **Daniele Romano**[2]

[1] *Unit of Electrical Engineering, University Campus Bio-Medico of Rome, Via Alvaro Del Portillo 21, Rome 00128, Italy*
[2] *UAq EMC Laboratory, Department of Industrial and Information Engineering and Economics, University of L'Aquila, Via G. Gronchi 18, L'Aquila 67100, Italy*

Correspondence should be addressed to Mauro Parise; m.parise@unicampus.it

Received 6 October 2019; Accepted 14 January 2020; Published 5 February 2020

Academic Editor: Paolo Baccarelli

This work presents a series representation for the mutual inductance of two coaxial pancake coils which remains accurate in non-quasi-static regime under the hypothesis that the current in the source coil is uniformly distributed. Making use of Gegenbauer's addition theorem and a term-by-term analytical integration, the mutual inductance between two generic turns belonging to distinct coils is expressed as a sum of spherical Hankel functions with algebraic coefficients. The accuracy and efficiency of the resulting expression is proved through pertinent numerical examples.

1. Introduction

Over the last decades, wireless power transfer (WPT) systems have attracted the interest of researchers working in a variety of scientific fields [1–11]. In fact, WPT systems find application in automotive battery [1] and consumer electronics' charging [2], in pacemaker battery charging [3], and in inductive links for low-power three-dimensional (3-D) integration systems [4]. Among all the WPT technologies, the magnetic resonance coupling (MRC) method is the one that offers better performances in terms of transfer distance and efficiency. In particular, previous authors have experimentally shown that efficiency of MRC-WPT is still reasonable even if transfer distance is slightly less than 10 times the radius of the coils [9].

In the past years, an analytical formula has been presented that allows predicting the magnetic coupling of two coaxial circular pancake coils [12]. However, the derived expression for the mutual inductance has the disadvantage of being in an integral form and, furthermore, of being tailored to the quasistatic frequency range only. As such, it can be used only if the effects of the displacement currents are negligible. Hence, when the operating frequency exceeds a few tens of MHz, like in ISM Band applications, the overall size of the whole two-coil system may not be any longer small enough for electromagnetic retardation to have negligible effect on the field distribution, and the quasistatic approximation fails.

The scope of this work is to derive a series representation for the mutual inductance of two coaxial pancake coils, which is valid in both the quasistatic and non-quasistatic frequency ranges of the two-coil system, provided that the current in the source coil may be assumed to be uniformly distributed. This occurs up to the frequency at which the length of the wire that constitutes the coil is approximately one-third of the free-space wavelength [13–16]. The expression comes from applying the integral form of Gegenbauer's addition theorem to the semi-infinite integral representation for the mutual inductance between two generic turns belonging to distinct coils. This permits to convert the product of Bessel functions of the integrand into the finite integral of a single Bessel function. Next, the semi-infinite integration is carried out analytically, and the integrand of the remaining finite integral is expanded into a power series of the cosine of the integration variable. This makes it possible to perform term-by-term analytical integration and express the mutual inductance as a sum of spherical Hankel functions with algebraic coefficients. The obtained formula holds as long as the thin-wire assumption, underlying the present derivation, is valid. This means that the wire radius must be far smaller than the radii of the turns that constitute the pancake coils. The advantages of the derived expression in terms of accuracy and time cost are illustrated through numerical examples.

2. Theory

Consider two thin-wire, coaxial, perfectly aligned, pancake coils separated by the distance d, as shown in Figure 1. The coils are made up of circular concentric loops connected in series, and it is assumed that the length of the wire connections between adjacent turns is much smaller than the length of the turn. Under this hypothesis, the coils may be regarded as composed of perfect and closed loops. If we denote by a_i ($i = 1, \ldots, N_a$) the radii of the turns of the lower coil and by b_j ($j = 1, \ldots, N_b$) the radii of the turns of the upper coil, the flux linkage per unit current between the coils may be expressed as

$$M_{\text{tot}} = \sum_{i=1}^{N_a} \sum_{j=1}^{N_b} M\left(a_i, b_j\right), \tag{1}$$

where $M(a, b)$ is the mutual inductance of two generic turns with radii a and b.

The purpose of this section is to exactly evaluate the complete integral representation for $M(a, b)$, given by [12].

$$M(a, b) = \pi\mu_0 ab \int_0^\infty \frac{e^{-u_0 d}}{u_0} J_1\left(k_\rho a\right) J_1\left(k_\rho b\right) k_\rho \mathrm{d}k_\rho, \tag{2}$$

with $J_\nu(\cdot)$ being the νth-order Bessel function, and

$$\begin{aligned} u_0 &= \sqrt{k_\rho^2 - k_0^2}, \\ k_0^2 &= \omega^2 \mu_0 \varepsilon_0, \end{aligned} \tag{3}$$

where μ_0 and ε_0 are, respectively, the magnetic permeability and dielectric permittivity of free space. To accomplish this task, we first use the relation ([17], Eq. (11.41.17))

$$J_1\left(k_\rho a\right) J_1\left(k_\rho b\right) = \frac{1}{\pi} \int_0^\pi J_0\left(k_\rho q\right) \cos\phi \, \mathrm{d}\phi, \tag{4}$$

with

$$q = \sqrt{a^2 + b^2 - 2ab\cos\phi}, \tag{5}$$

so as to express (2) as

$$M(a, b) = \mu_0 ab \int_0^\pi \cos\phi \left[\int_0^\infty \frac{e^{-u_0 d}}{u_0} J_0\left(k_\rho q\right) k_\rho dk_\rho \right] \mathrm{d}\phi. \tag{6}$$

Sommerfeld identity can now be applied to the evaluation of the improper integral within the square brackets of (6). It reads ([18], p. 9, equation (24))

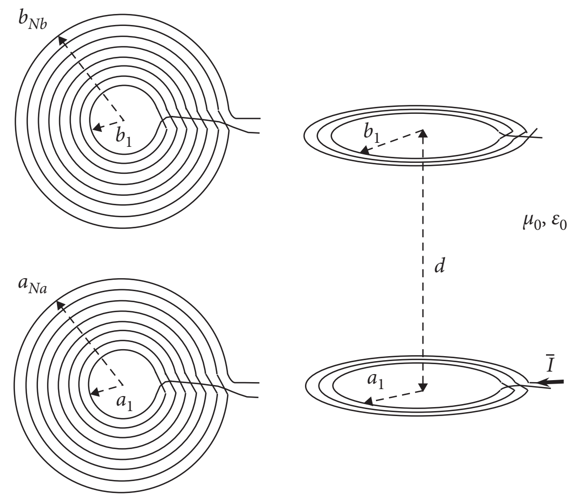

Figure 1: Sketch of two coaxial pancake coils.

$$\begin{aligned} \int_0^\infty \frac{e^{-u_0 d}}{u_0} J_0\left(k_\rho q\right) k_\rho dk_\rho &= \frac{e^{-jk_0\sqrt{q^2+d^2}}}{\sqrt{q^2 + d^2}}, \\ &= -jk_0 h_0^{(2)}\left(k_0\sqrt{q^2 + d^2}\right), \end{aligned} \tag{7}$$

where $h_l^{(2)}(\xi)$ is the lth-order spherical Hankel function of the second kind, and (6) is turned into

$$M(a, b) = -j\mu_0 k_0 ab \int_0^\pi g_0\left(k_0\sqrt{q^2 + d^2}\right) \cos\phi \, \mathrm{d}\phi, \tag{8}$$

with

$$g_n(\xi) = \frac{h_n^{(2)}(\xi)}{\xi^n}. \tag{9}$$

Upon setting

$$r^2 = a^2 + b^2 + d^2, \tag{10}$$

equation (8) may be rewritten as

$$M(a, b) = -j\mu_0 k_0 ab \int_0^\pi g_0\left(k_0\sqrt{r^2 + \tau}\right) \cos\phi \, d\phi, \tag{11}$$

where $\tau = -2ab\cos\phi$ and the analytical evaluation of the finite integral may be carried out once g_0, seen as a function of τ, is replaced with its Maclaurin expansion. It yields [19].

$$g_0\left(k_0\sqrt{r^2 + \tau}\right) = \sum_{n=0}^\infty \frac{1}{n!} \left(-\frac{k_0^2 \tau}{2}\right)^n g_n\left(k_0 r\right), \tag{12}$$

and (8) becomes

$$M(a, b) = -j\mu_0 k_0 ab \sum_{n=0}^\infty \frac{\left(k_0^2 ab\right)^n}{n!} g_n\left(k_0 r\right) \int_0^\pi \cos^{n+1}\phi \, \mathrm{d}\phi. \tag{13}$$

Finally, using the tabulated result ([20], Eqs. (2.512.2)–(2.512.3))

$$\int_0^{\pi} \cos^{n+1}\phi = \begin{cases} \pi n!!/(n+1)!!, & \text{odd } n, \\ 0, & \text{even } n, \end{cases} \tag{14}$$

makes it possible to obtain

$$M(a,b) = -j\pi\mu_0 k_0 ab \sum_{l=0}^{\infty} \frac{1}{2^{2l+1} l!(l+1)!} \left(\frac{k_0 ab}{r}\right)^{2l+1} h_{2l+1}^{(2)}(k_0 r), \tag{15}$$

where account has been taken of (9). Combining (15) and (1) provides a closed-form explicit expression for the mutual inductance between the two coaxial coils. In principle, the derived expression is valid for the considered coil geometry (see Figure 1), where the winding radius is approximately a piecewise constant function of the rotation angle around the coil axis and, as a consequence, it transits abruptly from the radius of one circular turn to the radius of the adjacent turn. However, previous authors [12] have shown that, for the purposes of inductance calculation, the coil geometry with concentric circular turns may be also used for modeling spiral-shaped coils. This may be performed especially when the turn-to-turn spacing is small if compared with the coil diameter (small coil pitch), which implies that the winding radius changes smoothly and slowly.

It should be observed that for long-distance wireless power transfer applications, which include the space solar power transmission systems [21] and the Internet of Things (IoT) [22], a simplified expression for $M(a,b)$ may be obtained. In fact, when the coil-to-coil spacing is large and the coils are electrically small the small-loop assumption holds, it is licit to take the limit of the sum in (15) as $a \longrightarrow 0$ and $b \longrightarrow 0$. This means retaining only the first term ($l = 0$) of the sum and letting $r \longrightarrow d$. It yields

$$M(a,b) = -\frac{j\pi\mu_0 (k_0 ab)^2}{2d} h_1^{(2)}(k_0 d), \tag{16}$$

and after substituting the identity [14, 23–26]

$$h_l^{(2)}(k_0 d) = j^{l+1} \frac{e^{-jk_0 d}}{k_0 d} \sum_{i=0}^{l} \frac{(l+i)!}{i!(l-i)!} (2jk_0 d)^{-i}, \tag{17}$$

one obtains the elementary expression:

$$M(a,b) = \frac{j\pi\mu_0 k_0}{2} \left(\frac{ab}{d}\right)^2 \left(1 + \frac{1}{jk_0 d}\right) e^{-jk_0 d}. \tag{18}$$

3. Numerical Results

As validation, the developed theory is applied to the computation of the amplitude of the mutual inductance between two coils made up of three turns, with radii $a_1 = b_1 = 4$ cm, $a_2 = b_2 = 6$ cm, and $a_3 = b_3 = 8$ cm. At first, the coil-to-coil spacing is assumed to be $d = 10$ cm, and the inductance is computed against frequency by using (1) in conjunction with (15), numerical integration of (2), and the well-known quasistatic solution in terms of complete elliptic integrals in [12]. In particular, numerical integration is performed by applying a G7-K15 Gauss–Kronrod quadrature scheme, arising from combining a 7-point Gauss rule with a 15-point Kronrod rule, while (15) is truncated at the index L, which is taken as a parameter. The obtained results, depicted in Figure 2, point out how the outcomes from the G7-K15 scheme perfectly agree with those resulting from (15) with $L = 4$. Instead, the quasistatic formula does not depend on frequency and as a consequence, can generate accurate results only in the low-frequency range, up to less than 10 MHz. Thereinafter, the whole two-coil system enters its non-quasi-static frequency region, where the effects of the displacement currents cease to be negligible. Thus, starting from about 10 MHz, the system is no longer small enough for electromagnetic retardation to have negligible effect on the field distribution.

A glance at the curves plotted in Figure 2 also allows concluding that expression (15) for the mutual inductance converges to the exact solution regardless of the operating frequency. Thus, if M is the exact value of the inductance at a given frequency and $\{M_L\}$ is the sequence of partial sums that originates from truncating (15) at the index L, it holds [27]

$$\lim_{L\longrightarrow\infty} \frac{|M_{L+1} - M|}{|M_L - M|^{\delta}} = c, \tag{19}$$

where $\delta \geq 1$ and c are, respectively, the order of convergence (OC) and the asymptotic error constant (AEC), which give information on the rate of convergence of $\{M_L\}$. Estimates of δ and c may be obtained by taking the limits of the sequences [27].

$$\delta_L = \frac{\log\left(|M_{L+1} - M_L| / |M_L - M_{L-1}|\right)}{\log\left(|M_L - M_{L-1}| / |M_{L-1} - M_{L-2}|\right)}, \tag{20}$$

$$c_L = \frac{|M_{L+1} - M_L|}{|M_L - M_{L-1}|^{\delta_L}}, \tag{21}$$

as $L \longrightarrow \infty$. As an example, Table 1 shows the values of δ_L and c_L when L is comprised between 5 and 9, calculated for the considered geometrical configuration at the operating frequency of 30 MHz.

As can be observed, as L is increased, the estimate δ_L of the order of convergence approaches unity, thus suggesting that the sequence of partial sums in (15) converges linearly. In addition, the small value of the asymptotic error constant contributes to accelerate the convergence of the proposed solution, since it implies a significant reduction of the remainder $M - M_L$ at any further iteration of the sequence $\{M_L\}$.

Accuracy being equal, use of (15) in place of the Gauss–Kronrod scheme allows reducing significantly the computation time. This aspect is illustrated by Table 2, which shows the average CPU time taken by the two approaches to calculate the amplitude-frequency spectra of M depicted in Figure 2. Table 2 also shows the ratio of the time taken by numerical integration to that required by (15), that is, the speed-up exhibited by the new method. As is seen, using the new method with $L = 10$ instead of the Gauss–Kronrod scheme permits to reduce the time cost by at least 20 times.

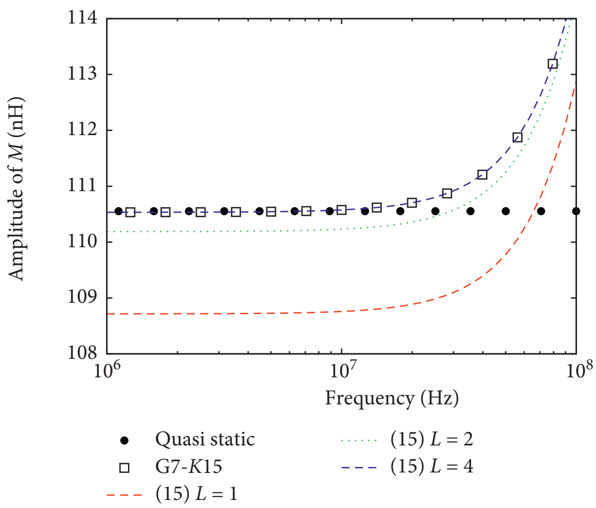

Figure 2: Mutual inductance between two pancake coils separated by the distance, $d = 10$ cm, calculated versus frequency.

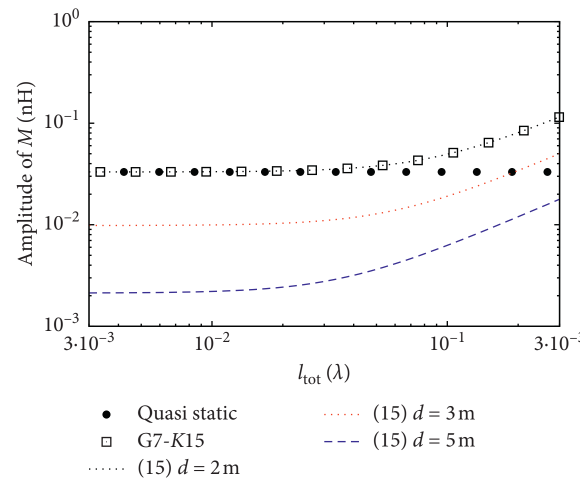

Figure 3: Mutual inductance between two pancake coils against the total wire length l_{tot}, expressed in free-space wavelengths. Three different values for the coil-to-coil spacing are considered.

Table 1: Estimated OC and AEC for the sequence $\{M_L\}$.

L	δ_L	c_L
5	0.955	0.462
6	0.971	0.424
7	0.986	0.415
8	0.990	0.388
9	0.992	0.372

Table 2: CPU time comparisons for the computation of M.

Approach	Average CPU time (s)	Speed up
G7-K15 scheme	1.69	—
(15) with $L = 2$	$3.49 \cdot 10^{-6}$	$4.84 \cdot 10^{5}$
(15) with $L = 4$	$4.58 \cdot 10^{-5}$	$3.69 \cdot 10^{4}$
(15) with $L = 6$	$7.26 \cdot 10^{-4}$	$2.33 \cdot 10^{3}$
(15) with $L = 10$	$8.12 \cdot 10^{-2}$	20.8

It should be noted that (2) and, as a consequence, the developed theory, is valid, subject to the condition that the current in the source coil is uniform, which, in general, is a reasonable assumption as long as the total length of the wire that constitutes the coil is less than $\lambda/3$, with λ being the free-space wavelength [13]. This implies an upper limit on the frequency range of validity of (15), which, however, is always greater than the limit of validity of the quasi-static field assumption underlying the previously published approach [12]. This aspect is illustrated in Figure 3, which depicts profiles of the amplitude of M as a function of the total wire length l_{tot} of the source coil, expressed in free-space wavelengths. The curves have been obtained by using (15), Gauss–Kronrod integration of (2), and the quasi-static approach, assuming the same two-coil system as in the preceding example. Three distinct values for the coil-to-coil spacing d are considered.

As is evident from the data in Figure 3, the exact curve arising from (15) and numerical integration of (2) start to deviate from the quasistatic trend when $l_{\text{tot}} \cong 0.02\lambda$, that is, well before the failure of the assumption of electrically small coil. The plotted curves also point out that the upper frequency limit of validity of the quasistatic assumption decreases as the distance d between the coils is increased. This is expected since, as d is increased, the frequency at which λ becomes comparable to it diminishes. The effect of changing d on the accuracy of the quasistatic solution may be better understood by taking a glance at Figure 4, which depicts d–profiles of $|M|$ arising from both the solutions in [12] and (15). The geometrical configuration is still the same as in the previous examples, and different operating frequencies are considered. As is noticed, for small values of d, the results from the quasistatic approach and (15) are overlapping, regardless of the operating frequency. Conversely, as the distance d grows up, the exact solution becomes more and more sensitive to frequency changes, and the discrepancy between any exact curve and the quasistatic trend becomes more and more pronounced. Since the data in Figure 4 are in logarithmic scale, this implies that

$$\log \frac{\left|M_{(15)}\right|}{\left|M_{qs}\right|} = g(d), \tag{22}$$

where $g(d)$ is an increasing function of d. Equation (22) makes it possible to acquire information on the relative error ε_R arising from using the quasistatic approach instead of the proposed one. In fact, from (22), it is found that

$$\varepsilon_R = \frac{\left|M_{(15)}\right| - \left|M_{qs}\right|}{\left|M_{(15)}\right|} = 1 - 10^{-g(d)}, \tag{23}$$

which suggests that the relative percent error generated by the quasistatic approach asymptotically approaches 100% as d grows up. This conclusion is confirmed by Figure 5, which shows plots of the relative error against d, with the operating frequency taken as a parameter.

As is seen, the slopes of the error curves are steepest for low values of d and dramatically reduce as d is increased. Finally, they tend asymptotically to zero as soon as the error approaches unity.

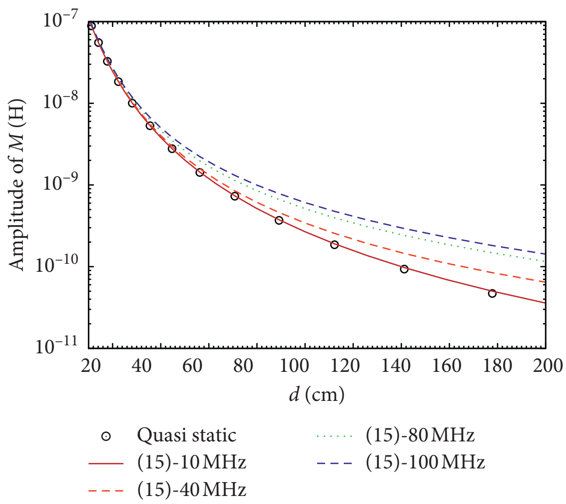

FIGURE 4: Mutual inductance between two pancake coils against the axial distance d, calculated by taking the operating frequency as a parameter.

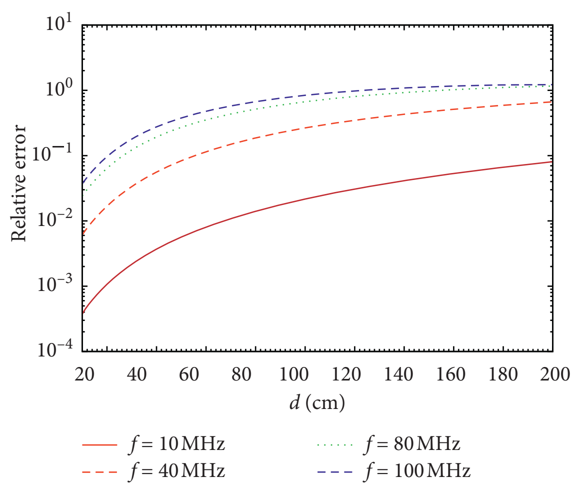

FIGURE 5: Relative error of the quasistatic approximation as compared with (15), computed against d.

4. Conclusion

In this work, a series solution for the mutual inductance of two coaxial pancake coils is presented. The Gegenbauer addition theorem and term-by-term analytical integration allows expressing the mutual inductance between two generic turns belonging to distinct coils as a sum of spherical Hankel functions with algebraic coefficients. Numerical tests are performed to confirm the accuracy of the proposed formula and to illustrate its advantages in terms of computation time over standard numerical techniques that may be used to calculate the mutual inductance.

Data Availability

The data used to support the findings of this study are included within the article.

Conflicts of Interest

The authors declare that they have no conflicts of interest.

References

[1] T. Imura, H. Okabe, and Y. Hori, "Basic experimental study on helical antennas of wireless power transfer for electric vehicles by using magnetic resonant couplings," in *Proceedings of the 2009 IEEE Vehicle Power and Propulsion Conference*, pp. 936–940, Dearborn, MI, USA, September 2009.

[2] Y. Yungtaek Jang and M. M. Jovanovic, "A contactless electrical energy transmission system for portable-telephone battery chargers," *IEEE Transactions on Industrial Electronics*, vol. 50, no. 3, pp. 520–527, 2003.

[3] C. Xiao, D. Cheng, and K. Wei, "An lcc-c compensated wireless charging system for implantable cardiac pacemakers: theory, experiment, and safety evaluation," *IEEE Transactions on Power Electronics*, vol. 33, no. 6, pp. 4894–4905, 2018.

[4] T. Vali, G. Marotta, L. De Santis, G. Antonini, D. Romano, and G. De Luca, "Full-wave modeling of inductive coupling links for low-power 3d system integration," in *Proceedings of the 2013 IEEE International Symposium on Electromagnetic Compatibility*, pp. 17–21, Denver, CO, USA, August 2013.

[5] M. Parise, V. Tamburrelli, and G. Antonini, "Mutual impedance of thin-wire circular loops in near-surface applications," *IEEE Transactions on Electromagnetic Compatibility*, vol. 61, no. 2, pp. 558–563, 2019.

[6] L. Jianyu, T. Houjun, and G. Xin, "Frequency splitting analysis of wireless power transfer system based on t-type transformer model," *Elektronika Ir Elektrotechnika*, vol. 19, no. 10, pp. 109–113, 2013.

[7] M. Parise, "On the use of cloverleaf coils to induce therapeutic heating in tissues," *Journal of Electromagnetic Waves and Applications*, vol. 25, no. 11-12, pp. 1667–1677, 2011.

[8] M. Parise, "A study on energetic efficiency of coil antennas used for RF diathermy," *IEEE Antennas and Wireless Propagation Letters*, vol. 10, pp. 385–388, 2011.

[9] Y. Chung, T. Lee, and S. Y. Lee, "Characteristic comparison of different resonators to extend transfer distance in superconducting wireless power transfer for electric vehicle using high temperature superconducting resonance coil," *Journal of International Council on Electrical Engineering*, vol. 7, no. 1, pp. 249–254, 2017.

[10] M. Parise, "An exact series representation for the EM field from a circular loop antenna on a lossy half-space," *IEEE Antennas and Wireless Propagation Letters*, vol. 13, pp. 23–26, 2014.

[11] M. Parise, "On the surface fields of a small circular loop antenna placed on plane stratified earth," *International Journal of Antennas and Propagation*, vol. 2015, Article ID 187806, 8 pages, 2015.

[12] C. M. Zierhofer and E. S. Hochmair, "Geometric approach for coupling enhancement of magnetically coupled coils," *IEEE Transactions on Biomedical Engineering*, vol. 43, no. 7, pp. 708–714, 1996.

[13] C. A. Balanis, *Antenna Theory: Analysis and Design*, John Wiley & Sons, New York, NY, USA, 4th edition, 2016.

[14] D. H. Werner, "An exact integration procedure for vector potentials of thin circular loop antennas," *IEEE Transactions on Antennas and Propagation*, vol. 44, no. 2, pp. 157–165, 1996.

[15] P. L. Overfelt, "Near fields of the constant current thin circular loop antenna of arbitrary radius," *IEEE Transactions on Antennas and Propagation*, vol. 44, no. 2, pp. 166–171, 1996.

[16] M. Parise, "Full-wave analytical explicit expressions for the surface fields of an electrically large horizontal circular loop antenna placed on a layered ground," *IET Microwaves, Antennas & Propagation*, vol. 11, no. 6, pp. 929–934, 2017.

[17] G. N. Watson, *A Treatise on the Theory of Bessel Functions, Ser. Cambridge Mathematical Library*, Cambridge University Press, Cambridge, UK, 1944.

[18] A. Erdelyi, *Tables of Integral Transforms*, McGraw-Hill, New York, NY, USA, 1954.

[19] M. Parise and G. Antonini, "On the inductive coupling between two parallel thin-wire circular loop antennas," *IEEE Transactions on Electromagnetic Compatibility*, vol. 60, no. 6, pp. 1865–1872, 2018.

[20] I. S. Gradshteyn and I. M. Ryzhik, *Table of Integrals, Series, and Products*, A. Jeffrey and D. Zwillinger, Eds., Academic Press, New York, NY, USA, 2007.

[21] M. M. Tentzeris, R. Vyas, W. Wei et al., "Power issues in biomedical telemetry," in *Handbook of Biomedical Telemetry*, K. S. Nikita, Ed., pp. 130–311, Wiley-IEEE Press, Piscataway, NJ, USA, 2014.

[22] C. T. Rim and C. Mi, *Wireless Power Transfer for Electric Vehicles and Mobile Devices*, John Wiley & Sons, New York, NY, USA, 2017.

[23] M. Parise, "Second-order formulation for the quasi-static field from a vertical electric dipole on a lossy half-space," *Progress In Electromagnetics Research*, vol. 136, pp. 509–521, 2013.

[24] M. Parise, "Exact EM field excited by a short horizontal wire antenna lying on a conducting soil," *AEU-international Journal of Electronics and Communications*, vol. 70, no. 5, pp. 676–680, 2016.

[25] M. Parise, "Efficient computation of the surface fields of a horizontal magnetic dipole located at the air-ground interface," *International Journal of Numerical Modelling: Electronic Networks, Devices and Fields*, vol. 29, no. 4, pp. 653–664, 2016.

[26] M. Parise, M. Muzi, and G. Antonini, "Loop antennas with uniform current in close proximity to the earth: canonical solution to the surface-to-surface propagation problem," *Progress in Electromagnetics Research B*, vol. 77, pp. 57–69, 2017.

[27] A. S. Householder, *The Numerical Treatment of a Single Nonlinear Equation*, McGraw-Hill, New York, NY, USA, 1970.